Journal of Mining and Environment (JME) Vol. 17, No. 5, 2026, 1945-1960

Shahrood University of Technology

Journal of Mining and Environment (JME)

Journal homepage: www.jme.shahroodut.ac.ir

Iranian Society of Mining Engineering (IRSME)

A 3D Geochemical Zonality Index Based on Staged Factor Analysis and Fractal Modeling in Porphyry Cu–Mo ore Deposits

Hassan Feizi Anhar[1], Ali Imamalipour[1*] and Peyman Afzal[2]

1. Department of Mining Engineering, Urmia University, Urmia, Iran
2. Department of Mining Engineering, South Tehran Branch, Islamic Azad University, Tehran, Iran

Article Info

Received 15 September 2025

Received in Revised form 2 November 2025

Accepted 31 December 2025

Published online 31 December 2025

DOI: 10.22044/jme.2025.16830.3300

Keywords

Enhanced geochemical zoning index

Staged Factor Analysis (SFA)

Fractal modeling

Porphyry Cu–Mo

3D modeling

Abstract

Geochemical zoning is a key concept in exploration geochemistry. It provides an effective means of predicting the erosion level of mineralization, distinguishing supra-ore from sub-ore halos, and identifying concealed ore bodies. While classical geochemical zoning methods have been widely applied for decades, this study introduces an enhanced three-dimensional geochemical zoning model tailored for the Sungun porphyry deposit based on geochemical data obtained from 264 drill cores totaling 33,368 rock samples. The model is constructed using ratios of factors derived from Staged Factor Analysis (SFA) of ore-related major (Cu and Mo) and minor (Cd, Mn, Pb, Zn, and Ag) elements, and further refined through fractal modeling for classification. The fractal modeling method (C-V) clearly shows four distinct populations and three breakpoints, corresponding to supergene (0.9–1.4%), hypogene (0.6–0.9%), and oxidized zones (0.1–0.6%). The application of the method to the Sungun porphyry system demonstrates a strong spatial correlation between the zoning index, copper grade distribution, and alteration patterns. SFA effectively separates supra-ore and sub-ore elements, while fractal modeling enhances the robustness of zoning classification. Integration of the developed 3D zoning index with copper grade models reveals a clear structural relationship among alteration, geochemical ratios, and copper distribution. The proposed approach improves the resolution of porphyry deposit zoning, offering enhanced targeting accuracy and reducing risk in deep drilling exploration.

1. Introduction

Identification of primary geochemical halos is a fundamental strategy in exploration geochemistry for detecting mineral deposits situated near or beneath the surface [1]. A primary geochemical halo refers to a zone surrounding an ore body within the host rocks, where elemental concentrations become anomalously enriched due to ore-forming processes [2-3]. The geochemical characteristics of these halos provide essential insights for predicting deep-seated mineral resources, as they reflect the geochemical mechanisms governing ore deposition and mineralized body formation.

Various analytical techniques have been employed to characterize primary halos, including vertical geochemical zoning of elements [4-6], element ratios that vector toward mineralized zones [7-9], Pearce element ratios [1], [10-13], and alteration indices [14-22]. Beus and Grigoryan [2], followed by Grigoryan [23], introduced the Zonality Index based on major and minor ore-related elements, typically classified into supra-ore and sub-ore associations across different mineral deposit types. A crucial component of these methods involves defining the spatial distribution of individual elements and their inter-element relationships.

Three-dimensional modeling has also gained widespread application as an effective tool in deep mineral exploration [24-27]. 3D models of primary geochemical halos enable direct visualization of elemental distributions and provide valuable

Corresponding author: a.imamalipour@urmia.ac.ir (A. Imamalipour).

insights into ore-forming systems [28-29]. Such models are particularly advantageous in mineral deposit studies, as they extend geochemical zoning into three dimensions and improve understanding of vertical variations in ore systems.

Lithogeochemical datasets derived from drill cores are inherently nonlinear, necessitating nonlinear analytical approaches for reliable interpretation. Mathematical techniques, such as Multivariate Analysis and Fractal Analysis, have proven effective in refining geochemical interpretations. Multivariate analysis is widely applied to reduce numerous variables into a smaller set of factors, which in exploration geochemistry typically correspond to ore-related elemental associations [30-34]. Factor analysis has been extensively used to group paragenetically related elements, and the resulting factor scores serve as effective tools for modeling geochemical anomalies and mineralized zones [33], [35-36]. Yousefi et al. [37] further advanced this approach by developing Staged Factor Analysis (SFA), which enables qualitative evaluation of factor scores across different mineralization types, particularly within porphyry systems.

Fractal analysis, first introduced by Mandelbrot [38], provides a structural framework for interpreting geological datasets, especially geochemical data. Several fractal models have since been developed and applied to classify geochemical anomalies and mineralized zones, including number-concentration, concentration-area, concentration-perimeter, concentration-distance, and concentration-volume models [38-42]. These methods explore relationships between elemental concentrations and the geometric properties of the space they occupy [32], [43-55].

In this study, the classical Zonality Index of Ziaii et al. [6] is refined by integrating SFA and fractal modeling within the Sungun porphyry copper system in northwestern Iran. Ratios between supra-ore and sub-ore factors were computed and subsequently classified using fractal algorithms to delineate prospective zones. The results were compared with those obtained from the classical Zonality Index and further validated using independent geological evidence and drill core data. The primary objective of this research is to introduce an enhanced three-dimensional geochemical zoning index for porphyry systems, integrating SFA and fractal modeling to overcome limitations inherent in classical methods.

Staged Factor Analysis (SFA) represents a significant advancement in multivariate statistical techniques tailored for the complex nature of geochemical exploration datasets. Natural geological systems contain geochemical data influenced by multiple overlapping signals, including barren host rocks, weathering and secondary dispersion effects, anthropogenic contributions, and the primary mineralization signature of interest. SFA addresses this challenge through an iterative filtering process designed to improve the signal-to-noise ratio, isolating robust multi-element patterns directly linked to mineralization processes and enabling detection of subtle anomalies that may otherwise remain obscured [37].

Traditional geochemical zoning studies frequently rely on classical statistical analyses, which effectively describe frequency distributions but do not capture spatial structure, continuity, or the geometric complexity of geological processes. Many geological phenomena, including elemental enrichment and dispersion in ore systems, exhibit fractal or multifractal behavior, characterized by self-similarity and complexity across scales [38]. The concentration-volume (C-V) fractal model is a well-established approach in exploration geochemistry for quantitatively modeling spatial structure and objectively distinguishing geochemical populations influenced by different geological processes [33,36,39]. Accordingly, integrating SFA with fractal modeling enhances accuracy and clarity in geochemical zoning using raw drill-core data.

The novelty of this study lies in applying factor ratios of supra-ore and sub-ore elements within a 3D analytical framework, which enables a more precise delineation of mineralized zones and offers a robust methodology for deep exploration targeting in porphyry Cu–Mo systems.

Recent developments in porphyry Cu geochemical zonation emphasize advanced fractal modeling approaches. Ghannadpour [56] applied the C-V fractal method to differentiate supergene, hypogene, and oxidized zones in porphyry copper systems, demonstrating the capability of fractal thresholds to objectively classify mineralization domains and highlight grade variations. This work underscores the potential of fractal methods in resolving ore distribution patterns and reinforces the significance of nonlinear techniques in deep exploration.

Similarly, Sadigh [57] investigated spatial distribution trends in porphyry copper deposits using combined fractal and spatial analyses, emphasizing the influence of multiscale structural controls on mineralization. The study revealed that fractal clustering patterns and spatial anisotropy

provide meaningful indicators of ore-forming processes in porphyry environments. By correlating structural trends with geochemical behaviors, this work demonstrates the value of integrating spatial metrics with geochemical models to enhance exploration targeting.

2. Geological setting

The Sungun porphyry copper deposit is situated approximately 100 km northeast of Tabriz in northwestern Iran. The related porphyry stock intrudes the Sungun anticline as well as surrounding Cretaceous limestones and Eocene volcanic–pyroclastic sequences, which vary compositionally from andesite to trachyte. Petrographic and geochemical evidence suggest that the Sungun intrusion represents a composite stock composed of an early monzonite–quartz monzonite phase, followed by younger dioritic and granodioritic intrusions [58]. Copper mineralization is predominantly associated with potassic and phyllic hydrothermal alteration. Field observations and petrographic analyses indicate emplacement of the Sungun stock through multiple intrusive pulses, each accompanied by hydrothermal activity.

Early hydrothermal alteration generated a central potassic assemblage characterized by orthoclase and biotite. Propylitic alteration developed coevally with potassic alteration but was restricted to the outer margins of the stock, whereas phyllic alteration formed during later stages and overprinted earlier assemblages [58]. The Sungun deposit hosts more than 500 Mt of Cu–Mo sulfide ore and lies within the northwestern sector of the Cenozoic magmatic arc of Iran, also referred to as the Urmia–Dokhtar or Sahand–Bazman magmatic belt trending NW–SE [59–61]. Most major porphyry copper systems in Iran, including Sarcheshmeh, Sungun, Miduk, and Darrehzar, are situated along this belt [62].

Geological mapping of the Sungun deposit (Figure 1) reveals a clear spatial relationship between porphyry intrusions and copper mineralization. Quartz monzonite porphyry bodies dominantly occupy the southern and western parts of the system, enveloping other intrusive phases, while Cretaceous limestones and associated skarn zones confine the porphyries to the north and east. Andesitic dikes are primarily developed in the northern and western sectors, mostly peripheral to the main intrusive stock. Skarn alteration and related mineralization are most prominent along the eastern contact zone of the intrusion [58][63].

Three genetically distinct types of sulfide mineralization have been recognized at Sungun: hypogene, contact metasomatic (skarn), and supergene enrichment. Hypogene mineralization formed concomitantly with potassic alteration and, to a lesser degree, during subsequent phyllic alteration, occurring primarily as disseminations and vein-hosted sulfides. Within the potassic zone, copper mineralization consists predominantly of chalcopyrite with subordinate bornite, whereas later-stage hypogene assemblages are chiefly chalcopyrite. Copper grades increase toward the outer portions of the central potassic core, ranging from <0.20 wt.% up to ~ approximately 0.85 wt.%. Maximum pyrite abundance (3–10 vol.%) occurs within the marginal quartz–sericite (phyllic) alteration zone. A well-developed supergene enrichment blanket is present in the upper part of the deposit, accompanied by deep clay alteration of feldspars [64].

3.Materials and methods

3.1. Zonality Index

Geochemical zonation represents a fundamental method for assessing erosion levels in mineral deposits and guiding the exploration of concealed ore bodies. Observations indicate that the spatial distribution (3D) of trace elements and mineral phases, either within primary geochemical halos or inside the ore bodies themselves, may exhibit either symmetrical or asymmetrical zoning patterns. Geochemical zoning within a halo is inherently vectorial, allowing classification of zoning types based on the chosen directional orientation. Beus and Grigoryan [2] identified three principal types of directional geochemical zoning within hydrothermal aureoles: axial, longitudinal, and transverse. Zonation aligned with the flow direction of ore-forming fluids is referred to as axial or vertical zonation.

The formation of porphyry copper deposits is closely linked to the upward migration of magmatic bodies and their associated hydrothermal fluids. Consequently, alteration and mineralization are predominantly concentrated in the upper portions of sub-volcanic stock porphyries and adjacent volcanic country rocks. This vertical fluid migration establishes a correspondence between axial and vertical zonation. Computation of vertical zonation indices (Vz) for specific deposits, using selected indicator elements, enables the assessment of erosion levels, estimation of residual mineralization, and delineation of primary halos (supra-ore, upper-ore, ore, lower-ore, and sub-ore)

[6], [65]. These indices provide a quantitative evaluation of the current erosion state and serve as effective vectors in the search for concealed mineralized zones.

Beus and Grigoryan [2] introduced the Geochemical Zonality Index as a tool to discriminate primary mineralization and associated primary halos from secondary dispersion halos. This method has been successfully applied to various deposit types at both regional and local scales [66]. Primary geochemical halos arise from interactions between host rocks and ore-forming fluids, producing systematic variations in elemental concentrations that are detectable and quantifiable. Moreover, the geochemical zonality model functions as a robust index for mineral exploration and for classifying geochemical anomalies or mineralized zones. The Zonality Index is generally expressed as the ratio of supra-ore to sub-ore elements across different deposit types [67 - 70].

In the present study, porphyry Cu–Mo systems were selected as the primary target. The principal ore-forming elements in such systems are copper (Cu) and molybdenum (Mo), while zinc (Zn), lead (Pb), gold (Au), and silver (Ag) are also commonly mineralized in the peripheral zones of these deposits [2], [23], [68]. The classical zonality model has been further refined in this research through integration with multivariate statistical techniques, particularly Staged Factor Analysis (SFA), to enhance the classification of supra-ore and sub-ore element associations.

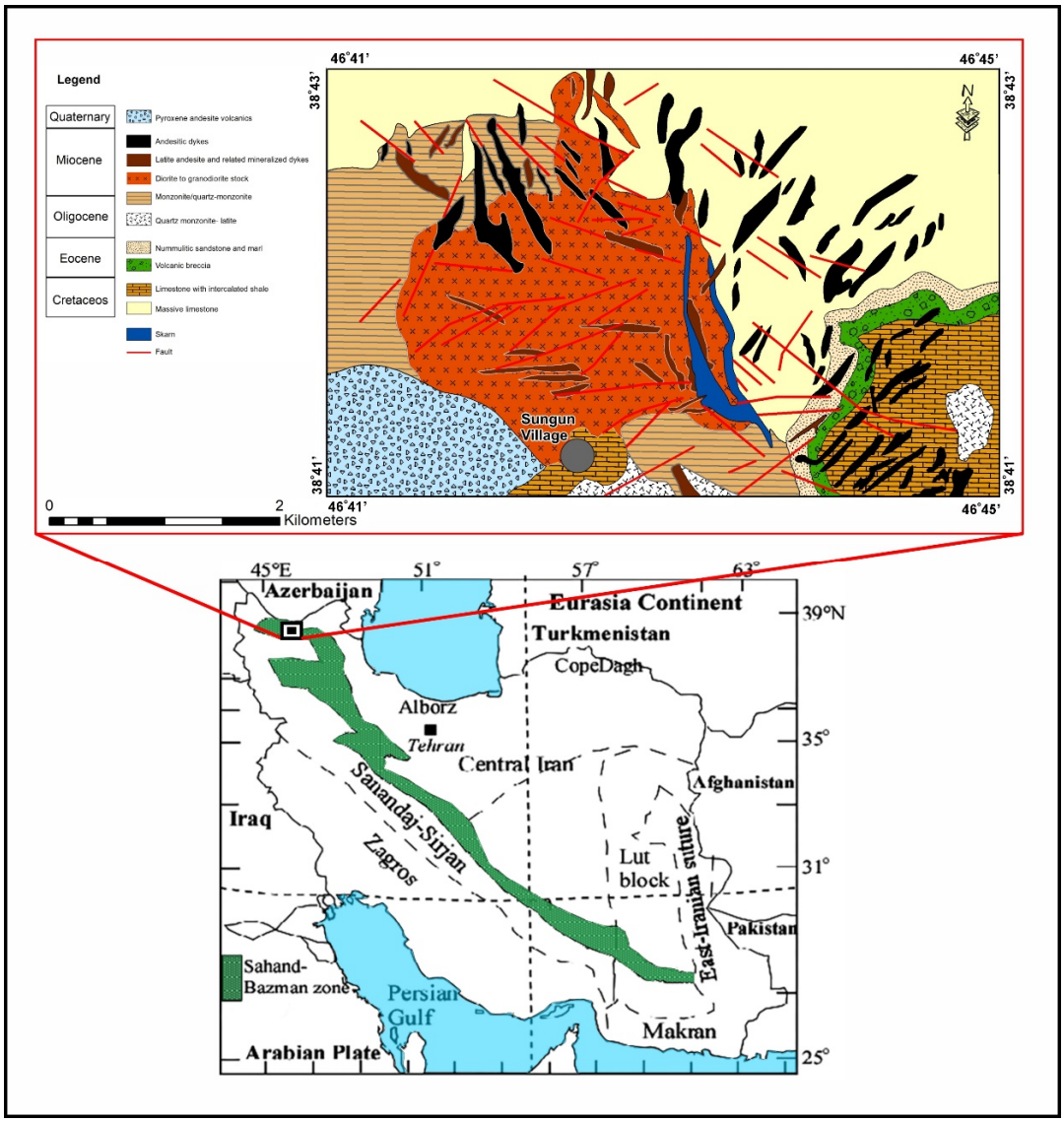

Figure 1. Geological map of Iran, showing the Urmia–Dokhtar (or Sahand–Bazman) magmatic belt, and the geological map of the Sungun deposit area [61][62][63]

3.2. Staged Factor Analysis (SFA)

Staged Factor Analysis (SFA) is a targeted multivariate technique specifically developed to identify multielement anomaly patterns across diverse mineral deposit types. In this approach, non-influential or noisy elements are progressively identified and removed through iterative stages, ultimately producing a robust geochemical pattern suitable for delineating mineralized zones [33], [37]. In the present study, before applying SFA, an isometric log-ratio (ilr) transformation was performed on the lithogeochemical drill-core data to enhance the reliability and precision of the multielement analysis [71].

Classical factor analysis with Varimax rotation was subsequently employed to extract geochemical factors, with a factor loading threshold of 0.5 used to segregate distinct element groups. Ratios between factors associated with primary ore-forming elements (Cu and Mo) and secondary ore-forming elements (Au, Ag, Pb, and Zn) were calculated to derive the zonality index. Furthermore, ratios of marginal elements to primary ore factors were computed to refine the index. Finally, the enhanced zonality index was classified using the concentration–volume (C–V) fractal model, enabling precise delineation of zones with the highest mineralization potential.

3.3. Fractal Grade–Volume Model

Cheng et al. [39] introduced the Concentration–Area (C–A) fractal model to separate geochemical anomalies from background values, analyzing the distribution of major, minor, and trace elements in the Mitchell–Sulphurets porphyry system, British Columbia, Canada. The model can be written as:

Equation 1:

$$A(\rho \le v) \propto \rho^{(-a1)}, A(\rho \ge v) \propto \rho^{(-a2)} \quad (1)$$

Where:

A ($\rho \le v$) and A ($\rho \ge v$) are the areas where element concentrations (ρ) are below or above the threshold v, respectively.

a1 and a2 are characteristic fractal exponents describing the scaling behavior.

Breakpoints in log–log plots of concentration versus area indicate thresholds separating distinct geochemical populations. Zou et al. [45] applied the C-A model to study vertical distributions of element concentrations in the Qulong Cu deposit, Tibet, China. Fractal models can describe vertical concentration features in mineralized and non-mineralized zones.

Cheng (2008) [44] showed that hydrothermal processes forming porphyry deposits often produce high metal concentrations with fractal or multifractal behavior. Cheng et al. [39] and Zou et al. [45] suggested extending the C-A model to volume, since elemental distributions in horizontal and vertical directions also follow fractal patterns.

Horizontal and vertical forms of the model: Equation 2 (Horizontal):

$$Ah(\rho \le v) \propto \rho^{(-a1)}, Ah(\rho \ge v) \propto \rho^{(-a2)} \quad (2)$$

Equation 3 (Vertical):

$$Av(\rho \le v) \propto \rho^{(-a1)}, Av(\rho \ge v) \propto \rho^{(-a2)} \quad (3)$$

Here:

Ah ($\rho \le v$) and Ah ($\rho \ge v$) are horizontal areas with concentrations below or above the threshold.

Av ($\rho \le v$) and Av ($\rho \ge v$) are vertical areas with concentrations below or above the threshold.

The Grade–Volume (C–V) fractal model expresses the distribution in 3D volume as:

Equation 4 (Volume):

$$V(\rho \le v) \propto \rho^{(-a1)}, V(\rho \ge v) \propto \rho^{(-a2)} \quad (4)$$

Where V ($\rho \le v$) and V ($\rho \ge v$) are volumes with concentrations below or above the threshold v, and a1 and a2 are the fractal exponents.

This method assumes that different regions in porphyry Cu deposits have fractal characteristics. Breakpoints in log–log plots of concentration versus volume separate distinct geochemical populations. In porphyry deposits, high-Cu areas occupy few voxels, while lower-Cu zones occupy many voxels in the 3D block model. C–V fractal thresholds therefore delineate mineralized zones from barren rocks.

For this study, drill-core concentrations were interpolated into a 3D block model using geostatistical kriging. Volumes V ($\rho \le v$) and V ($\rho \ge v$) were calculated as the number of voxels below or above the threshold multiplied by the voxel volume. Log–log plots were then used to analyze breakpoints and separate geochemical populations.

4. Discussion

4.1. Data

In this study, data from 264 drill holes, totaling 77,437 m in length, were utilized. From these cores, 33,368 rock samples were collected by the National Iranian Copper Industries Company and subsequently analyzed using ICP-MS. Geochemical investigations focused on Pb, Zn, Ag, Mn, Mo, Cu, and Cd, which were employed for

geochemical interpretation. Based on conventional statistical parameters, including skewness, kurtosis, and frequency distributions (Figure 2; Table 1), the datasets for the primary elements generally exhibited non-normal distributions.

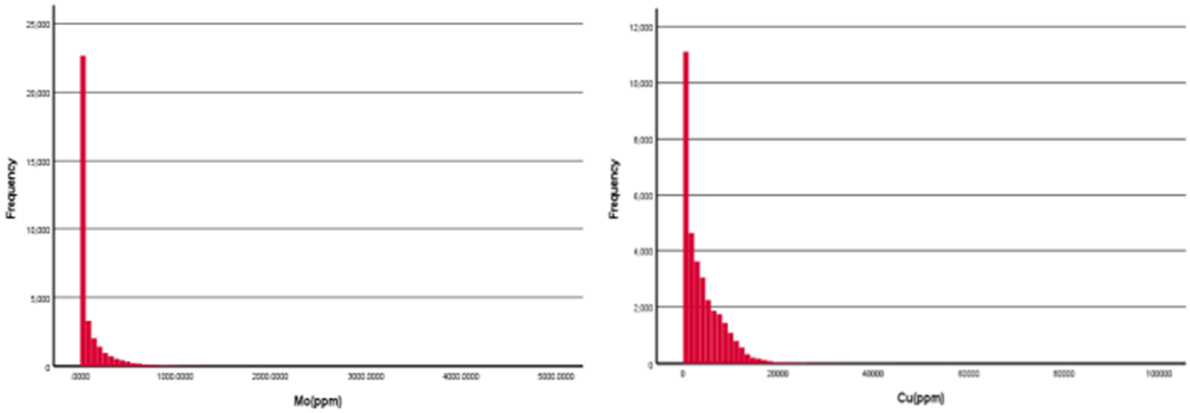

Figure 2. Histograms showing the distribution of copper (Cu) and molybdenum (Mo) concentrations in drill-core samples from the Sungun deposit.

Table 1. Statistical parameters of rock samples obtained from drill cores of the Sungun Cu porphyry deposit

Elements	Range	Minimum	Maximum	Mean	Standard Deviation	Variance	Skewness	Kurtosis
Ag (ppm)	80.499	0	80.5	0.85	1.64	2.69	17.44	557.05
Cd (ppm)	271.6	0.1	271.7	0.39	1.98	3.93	85.51	10736.72
Cu (ppm)	89381	1	89382	4001.4	4511.76	20355980.2	2.88	23.28
Mo (ppm)	4305.099	0.0009	4305.1	89.26	178.97	32030.29	4.69	42.79
Mn (ppm)	11584	5	11589	328.43	439.88	193497.03	5.97	83.65
Pb (ppm)	44190	2	44192	52.14	396.56	157256.07	58.72	5294.02
Zn (ppm)	66830.999	0.0009	66831	96.90	528.77	279597.44	72.56	8035.07

4.2. Multivariate Statistical Analysis

Initially, lithogeochemical data obtained from drill cores were normalized using a natural logarithm (Ln) transformation. Staged Factor Analysis (SFA) was then performed in three steps, as summarized in Table 2.

In the first step, calcium (Ca) was removed from the dataset. In the second step, factors associated with Cu–Mo porphyry-type mineralization were extracted, including factor F3-2, containing Ag, Cu, and Mo, and factor F4-2, containing Cd, Mn, Pb, and Zn. These factors were used as input for the third stage of analysis in Table 2.

In this final stage, primary ore-forming elements (Cu and Mo) were represented in factor F1-3, while secondary ore-forming elements (Cd, Mn, Pb, Zn, and Ag) appeared in factor F2-3. These secondary elements are mostly observed in the peripheral zones of the Cu–Mo porphyry system (Table 1). The factor loading plot from the final stage of analysis reveals two distinct factors, as illustrated in Figure 3.

4.3. 3D Geochemical–Fractal Zonality Modeling

In this study, the geochemical zonality index was calculated using an advanced approach. Unlike the traditional method, which relies on raw concentrations of supra-ore and sub-ore elements or their multiplicative ratios, the ratio between two factors representing supra-ore and sub-ore elements in porphyry deposits was employed, expressed as F_{2-3} / F_{1-3}. Additionally, a zonality index based on the element ratio (Pb × Zn) / (Cu × Mo) was computed for comparison with the factor-based ratio.

Subsequently, the Grade–Volume fractal model was applied to both indices. Log–log plots revealed four distinct geochemical populations for F_{2-3} / F_{1-3} and three populations for (Pb × Zn) / (Cu × Mo) (Figure 4). These populations were then used to define thresholds separating geochemical populations and to map mineralized zones in three dimensions.

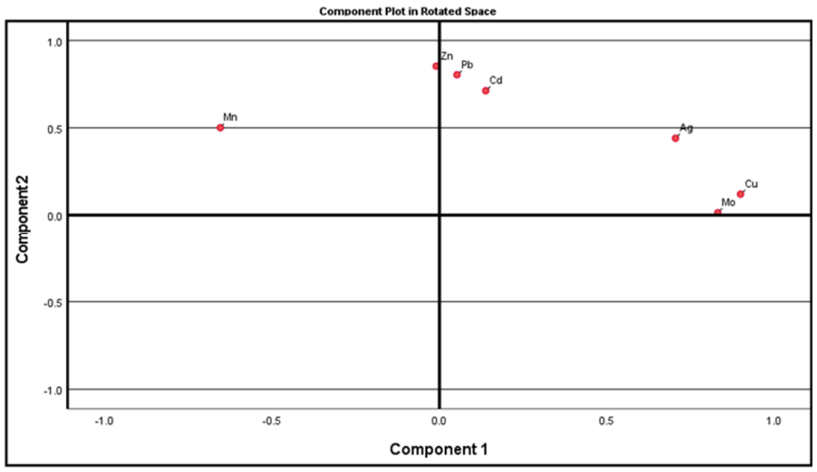

Figure 3. Factor loading plot of the final stage of SFA.

Table 2. Three steps of SFA were performed on rock sample data obtained from drill cores of the Sungun Cu porphyry deposit.

Rotated Component Matrix in first stage							Rotated Component Matrix in second stage							Rotated Component Matrix in third stage		
	Component							Component							Component	
	1	2	3	4	5	6		1	2	3	4	5	6		1	2
Ag	0.08	0.79	0.07	0.30	-0.24	0.16	Ag	0.09	0.07	0.78	0.33	-0.25	0.14	Ag	0.71	0.44
Al	0.83	-0.01	0.15	-0.21	0.13	0.04	Al	0.83	0.14	0.00	-0.21	0.12	0.04	Cu	0.90	0.12
As	-0.21	0.01	-0.04	0.27	-0.09	0.76	As	-0.22	-0.04	0.01	0.27	-0.07	0.78	Mo	0.83	0.01
Ca	0.44	-0.26	-0.13	0.35	-0.38	-0.22	Cd	-0.15	-0.08	0.16	0.59	-0.09	0.45	Cd	0.14	0.71
Cd	-0.15	0.17	-0.07	0.55	-0.07	0.49	Co	0.11	0.88	0.07	0.09	0.04	0.00	Mn	-0.65	0.50
Co	0.10	0.08	0.88	0.09	0.04	-0.01	Cr	0.83	0.17	-0.02	-0.15	-0.16	-0.14	Pb	0.05	0.80
Cr	0.83	-0.02	0.18	-0.16	-0.14	-0.12	Cu	-0.05	0.33	0.87	0.00	0.03	0.08	Zn	-0.01	0.85
Cu	-0.06	0.87	0.32	-0.02	0.03	0.07	Fe	0.16	0.80	0.03	0.16	-0.25	0.14			
Fe	0.16	0.04	0.80	0.14	-0.22	0.16	La	-0.16	-0.22	-0.04	0.12	0.83	-0.17			
La	-0.17	-0.05	-0.23	0.11	0.84	-0.15	Mn	0.25	-0.04	-0.53	0.61	-0.14	-0.10			
Mn	0.25	-0.50	-0.05	0.66	-0.18	-0.13	Mo	-0.20	-0.06	0.81	-0.01	0.14	-0.02			
Mo	-0.20	0.81	-0.06	-0.04	0.15	-0.02	Ni	0.46	0.71	0.14	-0.04	0.01	0.06			
Ni	0.46	0.14	0.71	-0.04	0.02	0.05	P	0.22	0.14	0.02	-0.17	0.76	0.08			
P	0.23	0.00	0.12	-0.13	0.74	0.03	Pb	-0.28	0.11	0.09	0.75	0.01	0.11			
Pb	-0.29	0.11	0.11	0.72	0.03	0.17	S	-0.15	0.64	0.56	-0.01	-0.08	0.10			
S	-0.15	0.56	0.63	0.00	-0.10	0.07	Sb	-0.09	0.26	0.12	0.04	-0.07	0.79			
Sb	-0.08	0.11	0.26	0.02	-0.07	0.78	Sc	0.90	-0.03	-0.08	-0.04	-0.09	-0.12			
Sc	0.90	-0.08	-0.03	-0.03	-0.09	-0.12	Th	-0.40	-0.16	0.04	0.10	0.77	-0.13			
Th	-0.39	0.03	-0.18	0.12	0.75	-0.15	V	0.91	0.04	-0.13	-0.09	-0.10	-0.19			
V	0.91	-0.13	0.05	-0.09	-0.08	-0.17	Y	0.79	0.08	-0.10	0.15	0.06	-0.04			
Y	0.79	-0.09	0.08	0.19	0.04	-0.08	Yb	0.66	0.27	-0.14	0.31	-0.24	-0.05			
Yb	0.65	-0.12	0.28	0.31	-0.24	-0.04	Zn	0.10	0.16	0.07	0.83	0.12	0.13			
Zn	0.09	0.10	0.17	0.81	0.13	0.17										

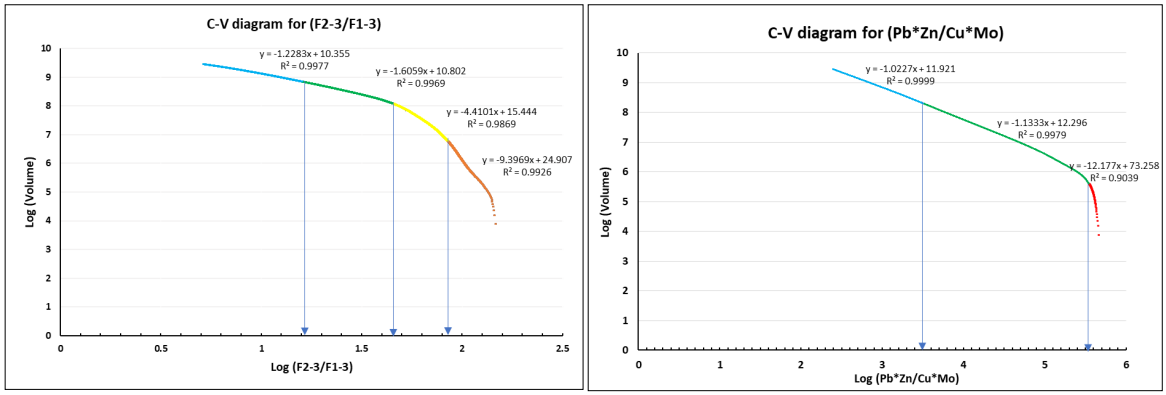

Figure 4. Log–Log Grade–Volume Curves for the Ratios F_{2-3} / F_{1-3} and (Pb × Zn) / (Cu × Mo).

Three-dimensional block models for the ratios F_{2-3} / F_{1-3} and (Pb × Zn) / (Cu × Mo) were generated using ordinary kriging in RockWorks 2017 (Figure 5). Each 3D model comprises 458,136 volumetric cells, with individual cell dimensions of 25 × 25 × 12.5 m along the X, Y, and Z axes, respectively.

Based on the log–log plots, the (Pb × Zn) / (Cu × Mo) ratio revealed three distinct statistical populations, with breakpoints at 3.5 and 5.54 (Figure 4). In contrast, the F_{2-3} / F_{1-3} ratio delineated four populations, with corresponding breakpoints at 1.2, 1.65, and 1.92 (Figure 4). These findings indicate that regions with lower ratio values exhibit substantial spatial overlap between the two indices in the volumetric fractal models.

Within the 3D volumetric models, the (Pb × Zn) / (Cu × Mo) ratio corresponds to 3,162 volumetric cells, whereas the F_{2-3} / F_{1-3} ratio corresponds to 16 cells (Figure 5). Despite this discrepancy, both indices demonstrate notable spatial overlap in the northern sector of the model. At higher ratio values, the F_{2-3} / F_{1-3} ratio (83 cells) displays greater dispersion and a higher density of volumetric cells relative to the (Pb × Zn) / (Cu × Mo) ratio (346,737 cells). Although the spatial distributions of the two indices differ, the northern portion of the 3D model continues to exhibit significant overlap between them (Figure 5).

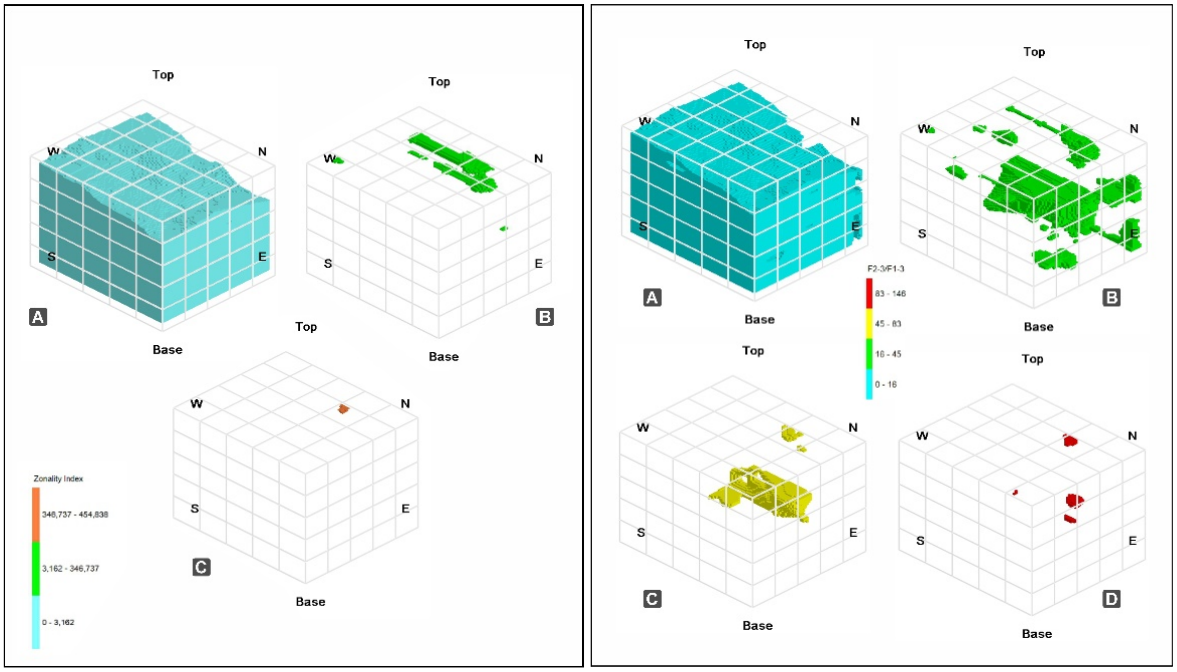

Figure 5. 3D spatial distribution of the ratios F_{2-3} / F_{1-3} and (Pb × Zn) / (Cu × Mo) based on the concentration–volume (C–V) fractal model, showing overlapping zones at lower values and more dispersed populations at higher values.

4.4. Copper Grade Modeling Using the Concentration–Volume (C–V) Fractal Method

To estimate the spatial distribution of copper grades within the Sungun deposit, ordinary kriging was performed using RockWorks 2017. The sub-block dimensions were defined as 25 × 25 × 12.5 m along the X, Y, and Z directions, respectively. Block sizes were determined following David's rule [72], which recommends sub-block dimensions between one-half and one-fourth of the drill-hole grid spacing. In this deposit, with an average drill spacing of 100 m during the detailed stage, the X and Y dimensions were set at 25 m, while the Z dimension, typical for metallic deposits, was defined as 12.5 m, approximately corresponding to the height of extraction benches.

Distinct geochemical populations, or zones, within the Sungun deposit were delineated using the concentration–volume (C–V) method. The Cu C–V curve reveals four distinct populations with three breakpoints (Figure 6), corresponding to copper grades of 0.6%, 0.9%, and 1.4%. The final, steep segment of the curve represents the highest-grade and most enriched population, indicative of the supergene enrichment zone. Based on the log–log plot, Cu grade ranges were assigned as follows: 0.9–1.4% for the supergene-enriched zone, 0.6–0.9% for the hypogene zone, and 0.1–0.6% for the oxidized zone (Figure 6).

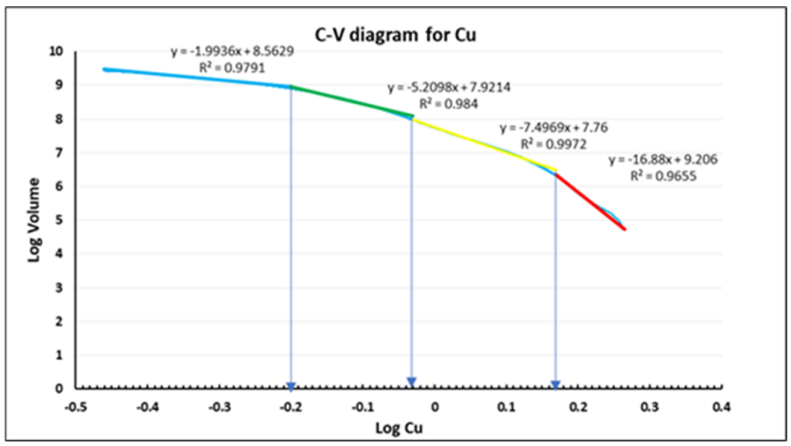

Figure 6. Log–log concentration–volume (C–V) curve for copper (Cu) grades in the Sungun deposit, showing four distinct populations and three breakpoints corresponding to the oxidized, hypogene, and supergene-enriched zones.

4.5. Integration of Alteration and Cu Grade Models

Alteration models are fundamental for defining zonal boundaries and providing geological context, as described by Lowell and Guilbert [73]. According to these models, phyllic and potassic alterations host the principal mineralization within the supergene-enriched and hypogene zones. Copper (Cu) mineralization patterns derived from the concentration–volume (C–V) method can be compared with geological data to validate results across different porphyry Cu deposits. It is reasonable to assume the existence of spatial correlations between modeled Cu zones and geological features such as mineralogy and alteration assemblages.

Three-dimensional geological models of the deposit were constructed using RockWorks™ 2017 and subsurface drill-hole data, including collar coordinates, dip, azimuth, lithology, alteration, and mineralogical information. Surface data, such as topography, faults, magmatic outcrops, and other relevant geological features, were incorporated to build the 3D models. The spatial relationship between Cu distribution and alteration zones is illustrated in Figs. 7 and 8.

3D alteration modeling reveals extensive phyllic and potassic alteration associated with the deposit (Figs. 8-B and 8-C), with phyllic alteration covering a larger area than potassic. The supergene-enriched zone, as defined by the C–V method, is concentrated in the southern and southeastern sectors of the deposit (Figure 7-C) and shows strong spatial correlation with phyllic and potassic alteration zones. Similarly, the hypogene zone obtained from the C–V model aligns with these alteration patterns, with the highest metal concentrations located in the central and southern portions of the deposit (Figure 7-B).

The log–log C–V plot (Figure 6) indicates Cu concentrations exceeding 1.4%, representing a potential new mineralization phase. This high-grade Cu phase is hosted within skarn units,

particularly in the southeastern sector of the deposit (Figure 7-D). The enriched Cu concentrations are entirely contained within the porphyry stock and correspond spatially with metamorphic skarn units (Figure 8-D). Consequently, the skarn units can be interpreted as hosts for elevated Cu concentrations, representing additional mineralization zones in the eastern and northern parts of the deposit. Geological observations confirm that a portion of the Cu mineralization occurs within these skarn units, as illustrated in Figure 7.

4.6. Three-Dimensional Modeling of the Developed Zonality Index (F_{2-3} / F_{1-3})

In this study, the zonality index was calculated as the ratio of supra-ore factor scores (F_{2-3}) to sub-ore factor scores (F_{1-3}). Lower index values correspond to areas dominated by Cu and Mo, coinciding with the potassic alteration zone. This relationship is clearly illustrated in the 3D block model, where minimum index values spatially align with high Cu grade zones and the potassic alteration domain (Figs. 5 and 8).

The 3D model of the developed zonality index (F_{2-3} / F_{1-3}) reveals a distinct spatial pattern associated with geochemical ratio distribution within the Sungun Cu porphyry system. Maximum index values are observed in near-surface portions of the system, primarily above the phyllic and propylitic alteration zones, although in some areas, elevated concentrations extend even above the potassic zone. This distribution reflects the influence of physicochemical conditions within the hydrothermal system and their variation with depth.

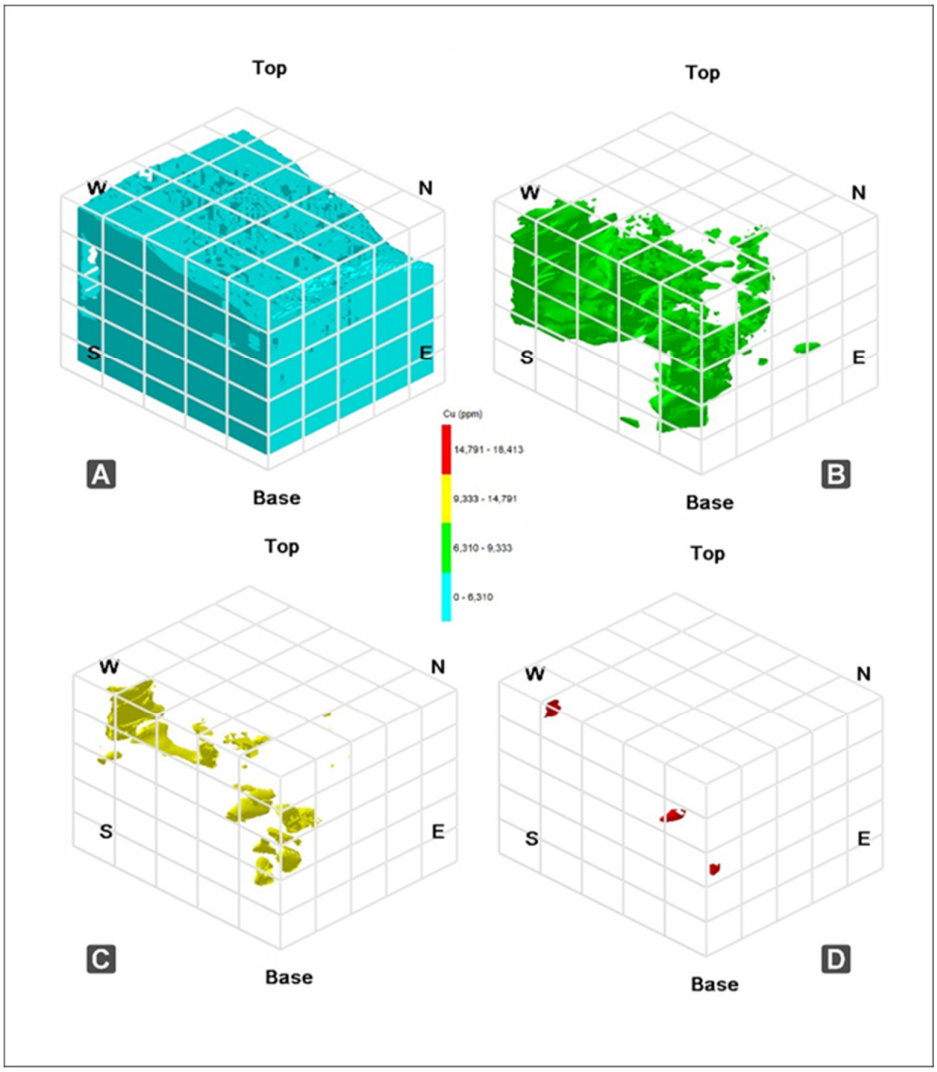

Figure 7. Concentration–volume (C–V) fractal models for Cu grades in different zones of the Sungun deposit: (A) oxidized zone, (B) hypogene zone, (C) supergene-enriched zone, and (D) skarn-associated zone, highlighting high-grade mineralization.

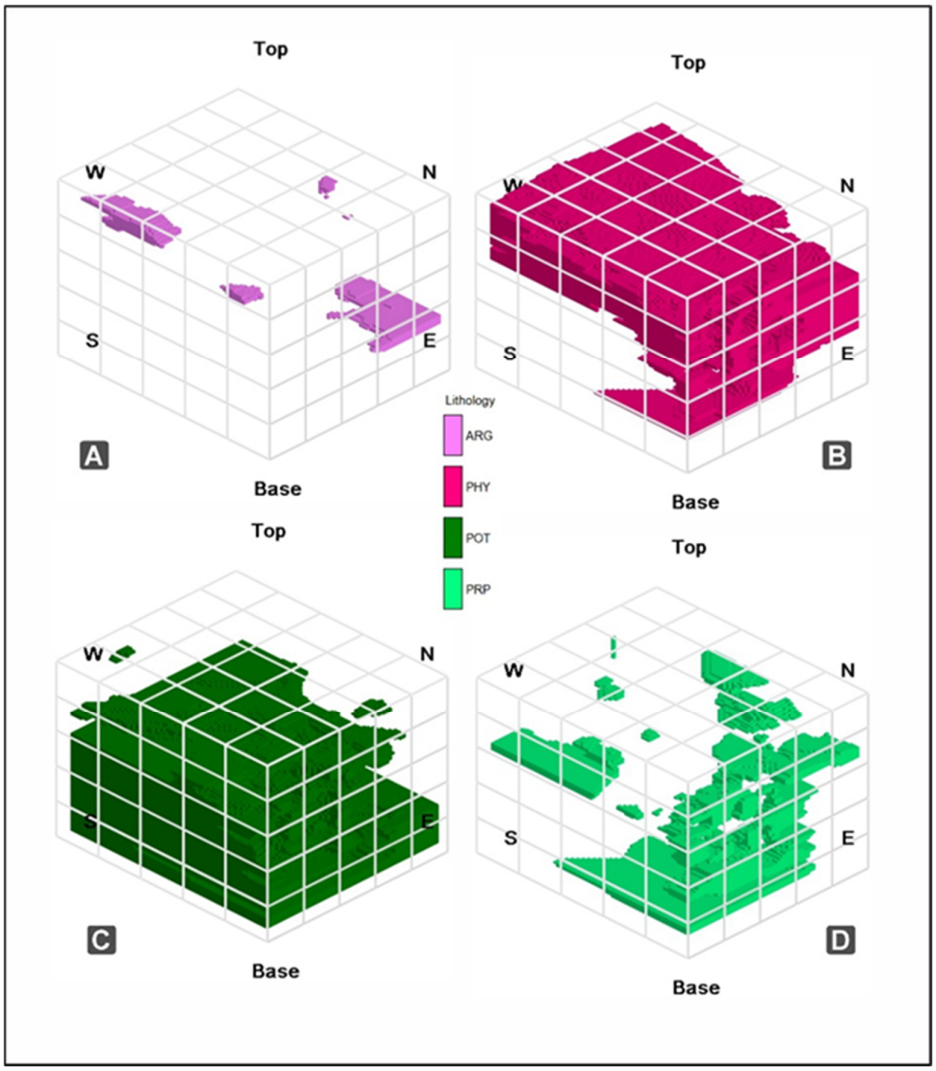

Figure 8. Three-dimensional alteration models of the Sungun Cu porphyry system: (A) argillic, (B) phyllic, (C) potassic, and (D) propylitic zones.

According to alteration models, the potassic zone occurs at greater depths and represents the principal Cu-mineralized region of the porphyry system. Comparison with the 3D Cu grade model indicates that the highest Cu concentrations are precisely located within this zone, while grades gradually decrease in overlying phyllic and propylitic zones. This pattern is consistent with established models of porphyry deposits, wherein temperature, pressure, and fluid composition at depth create optimal conditions for Cu deposition.

From a geochemical perspective, the increase in the F_{2-3} / F_{1-3} ratio near the surface may result from upward migration of associated elements via hydrothermal fluids, which undergo cooling and chemical modification. This mobilization concentrates supra-ore elements in the upper zones while relatively depleting Cu mineralization in these regions. Thus, analyzing these geochemical ratios in conjunction with known alteration patterns provides a detailed understanding of the porphyry system's structure and mineralization distribution. Variations in the developed zonality index with depth effectively reflect hydrothermal and geochemical processes within the system.

Furthermore, the 3D distribution of the zonality index is not perfectly concentric. Anomalies and dispersions, particularly in the northern sectors and around skarn contacts, suggest that the index is sensitive to more complex fluid pathways, potentially influenced by structural controls and overprinting of multiple hydrothermal events, which are common in porphyry systems.

5. Conclusions

This study aimed to develop a geochemical zonality index based on Staged Factor Analysis

(SFA) and to evaluate its applicability in conjunction with ore zone, alteration, and Cu grade models within a porphyry Cu system. SFA was performed on lithogeochemical drill-core data in three sequential steps to identify and remove noisy or ineffective elements. Ultimately, three end-factors, $F_{1–3}$ and $F_{2–3}$, were identified, representing primary ore-forming elements (Cu and Mo) and secondary ore-forming elements (Cd, Mn, Pb, Zn, and Ag), respectively. To calculate the developed geochemical zonality index, the ratio between these two factors ($F_{2–3}$ / $F_{1–3}$) was employed instead of relying on raw concentrations of supra-ore and sub-ore elements or their multiplicative ratios.

Log–log plots revealed that the (Pb × Zn) / (Cu × Mo) ratio delineated three distinct statistical populations, whereas the $F_{2–3}$ / $F_{1–3}$ ratio identified four populations. These results indicate that regions with lower ratio values exhibit significant overlap between the two indices in the volumetric fractal models, particularly in the northern parts of the 3D model. Based on concentration–volume (C–V) fractal modeling, distinct geochemical populations, or zones, within the Sungun deposit were separated. Breakpoints on the Cu C–V curve corresponded to Cu grades of 0.6%, 0.9%, and 1.4%, with grade ranges assigned as follows: 0.9–1.4% for the supergene enrichment zone, 0.6–0.9% for the hypogene zone, and 0.1–0.6% for the oxidized zone.

The results demonstrate that the developed zonality index effectively reflects geochemical and depth-dependent zoning within the porphyry system and serves as a robust tool for predicting the location of deep Cu mineralization, which likely corresponds to the potassic alteration zone. In porphyry copper systems, the ore zone (including supra-ore and lower-ore) coincides with the potassic zone; in other words, the potassic zone represents the central core of mineralization. Therefore, zonality index values that align with the ore zone can be interpreted as indicative of the potassic zone. Furthermore, the 3D model of the index shows strong spatial correspondence with alteration and Cu grade distributions, highlighting systematic relationships among alteration types, geochemical ratios, and metal concentrations. Integrating Cu grade models with the 3D zonality index, combined with advanced data analysis techniques, enables more precise zonation of porphyry deposits and can significantly enhance exploration targeting while reducing the risk associated with deep drilling.

While the validation presented herein, based on spatial correlation with copper grades and alteration zones, is robust, further mineralogical verification (e.g., detailed thin-section analysis and mineral chemistry studies) is recommended to strengthen the model in future research. We also suggest applying this method to additional porphyry deposits to test its robustness and potential for generalization across diverse geological settings and scales. Complementary validation approaches, such as success rate curves and P–A plots, may provide a more quantitative assessment of model performance beyond geological cross-validation.

It is important to note here that porphyry systems are dynamic and often deviate from a strictly concentric model.

Finally, it is important to note that porphyry systems are dynamic and often deviate from a strictly concentric model. We also believe that late mineralization and alteration overprinting, if they occur, can disrupt element distribution patterns and geochemical zonation patterns. The model used in this study is not based on a pre-defined, rigid concentric template. Instead, it is a data-driven approach that extracts patterns directly from the geochemical composition of the rocks. The Staged Factor Analysis (SFA) identifies the elemental associations ($F_{1–3}$ and $F_{2–3}$) that are most statistically significant within this specific deposit. If multiple hydrothermal pulses have overprinted each other, their geochemical signatures are blended in the final rock composition. The factors we use are the result of this entire history. Therefore, the $F_{2–3}$ / $F_{1–3}$ ratio inherently reflects the net effect of all fluid-rock interactions, including overprinting events.

Acknowledgment

This research was made possible with the aid of the office of the vice-chancellor for 'Research and Technology' at Urmia University and the National Iranian Copper Industries Company (NICICO) for the logistic support and providing access to the prospect and analytical data. We acknowledge their support.

References

[1]. Carranza, E. J. M., & M. Sadeghi., (2012). Primary geochemical characteristics of mineral deposits–implications for exploration. *Ore Geology Reviews, vol. 45*, pp. 1–4.

[2]. Beus, A. A., Grigoryan, S. V., (1977). Geochemical Exploration Methods for Mineral Deposits. Applied Publishing Ltd., Wilmette, Illinois.

[3]. Solovov, A. P., (1987). Geochemical Prospecting for Mineral Deposits. Mir, Moscow .

[4] Distler, V. V., Yudovskaya, M. A., Mitrofanov, G. L., Prokofiev, V. Y., & Lishnevskii, E. N. (2004). Geology, composition, and genesis of the Sukhoi Log noble metals deposit, Russia. *Ore Geology Reviews, vol. 24*, no. 1-2, pp. 7–44.

[5]. Gundobin, G. M., (, 1984) Peculiarities in the zoning of primary halos. *Journal of Geochemical Exploration, vol. 21*, no. 1-3, pp. 193–200.

[6]. Ziaii, M., Carranza, E.J.M., Ziaei, M., (2011). Application of geochemical zonality coefficients in mineral prospectivity mapping. *Comput. Geosci. 37*, 1935–1945.

[7]. Goodell, P. C., & Petersen, U., (1974). Julcani mining district, Peru: a study of metal ratios. *Economic Geology, vol. 69, no. 3*, pp. 347–361 .

[8]. Jones, B. K. (1992). Application of metal zoning to gold exploration in porphyry copper systems. *Journal of Geochemical Exploration, vol. 43*, no. 2, pp. 127–155 .

[9]. Pirajno, F., & Smithies, R. H. (1992). The FeO/(FeO+MgO) ratio of tourmaline: a useful indicator of spatial variations in granite-related hydrothermal mineral deposits. Journal of Geochemical Exploration, vol. 42, no. 2-3, pp. 371–381.

[10]. Pearce, T. H. (1968). A contribution to the theory of variation diagrams. *Contributions to Mineralogy and Petrology, vol. 19*, no. 2, pp. 142–157.

[11]. Stanley, C. R., & Madeisky, H. E. (1994). Lithogeochemical Exploration for Hydrothermal Ore Deposits Using Molar Element Ratio Analysis in Alteration and Alteration Processes Associated with Ore-Forming Systems. Geological Association of Canada, Short Course Notes, D. R. Lentz, Ed., vol. 11, pp. 193–211.

[12]. Urqueta, E., Kyser, T. K., Clark, A. H., Stanley, C. R., & Oates, C. J. (2009). Lithogeochemistry of the Collahuasi porphyry Cu, Mo, and epithermal Cu-Ag (Au) cluster, northern Chile: Pearce element ratio vectors to ore. Geochemistry: Exploration, Environment, *Analysis, vol. 9*, pp. 9–17.

[13]. Krein, M. G., & Melik-Adamjan, F. E. (2011). An integrated lithogeochemical approach to detecting and interpreting cryptic alteration around the Elura Zn-Pb-Ag deposit, New South Wales, Australia. Geochemistry: Exploration, Environment, *Analysis, vol. 11*, pp. 233–246.

[14]. Ishikawa, Y., Sawaguchi, T., Iwaya, S., & Horiuchi, M. (1976). Delineation of prospecting targets for Kuroko deposits based on modes of volcanism of underlying dacite and alteration haloes. *Mining Geology, vol. 26*, pp. 105–117 .

[15]. Date, J., Watanabe, T., & Saeki, Y. (1983). Zonal alteration around the Fukazawa kuroko deposits, Akita prefecture, northern Japan. *Economic Geology, vol. 5*, pp. 365–386.

[16]. Kishida, A., & Kerrich, R. (1987). Hydrothermal alteration zoning and gold concentration at the Kerr–Addison Archean lode gold deposit, Kirkland Lake, Ontario. *Economic Geology, vol. 82*, no. 3, pp. 649–690.

[17]. Barrie, C. T. (1993). Petrochemistry of shoshonitic rocks associated with porphyry copper-gold deposits of central Quesnellia, British Columbia, Canada. *Journal of Geochemical Exploration, vol. 48*, p. 258 .

[18]. Large, R. R., & Mcgoldrick, P. J. (2000). Lithogeochemical halos and geochemical vectors to stratiform sediment-hosted Zn-Pb-Ag deposits: HYC deposit, McArthur River, Northern Territory, Queensland. *Journal of Geochemical Exploration, vol. 68*, no. 1-2, pp. 105–126.

[19]. Large, R. R., McPhie, J., Gemmell, J. B., Herrmann, W., & Davidson, G. J. (2001). The spectrum of ore deposit types, volcanic environments, alteration halos, and related exploration vectors in submarine volcanic successions: some examples from Australia," *Economic Geology, vol. 96*, no. 5, pp. 913–938 .

[20]. Piche, M., & Jébrak, M. (2004). Normative minerals and alteration indices developed for mineral exploration. *Journal of Geochemical Exploration, vol. 82*, no. 1-3, pp. 59–77.

[21]. Prendergast, K. (2007). Application of lithogeochemistry to gold exploration in the St Ives Goldfield, Western Australia. Geochemistry: Exploration, Environment, *Analysis, vol. 7*, pp. 99- 108 .

[22]. Wang, L., Percival, J., Hedenquist, J. W., Hattori, K., & Qin, K. Z. (2021). Alteration mineralogy of the Zhengguang Au-Zn deposit, Northeast China: interpretation of shortwave infrared analyses during mineral exploration and assessment. Economic Geology, vol. 116, no. 2, pp. 389–406.

[23]. Grigoryan, S.V. (1992). Mining Geochemistry. Nedra Publishing House, Moscow (in Russian).

[24]. Kemp, E. A. D., Monecke, T., Sheshpari, M., Girard, E., & Bellefleur, G. (2011). 3D GIS as a support for mineral discovery. Geochemistry: Exploration, Environment, *Analysis, vol. 11*, pp. 117–128.

[25]. Hill, E. J., Oliver, N. H. S., Cleverley, J. S., Nugus, M. J., Carswell, J., & Clark, F. (2014). Characterisation and 3D modelling of a nuggety, vein-hosted gold ore body, Sunrise Dam, Western Australia. *Journal of Structural Geology, vol. 67*, pp. 222–234.

[26]. Wang, G., Zhang, S., Yan, C., et al. (2011). Mineral potential targeting and resource assessment based on 3D geological modeling in Luanchuan region, China.

Computers & Geosciences, vol. 37, no. 12, pp. 1976–1988.

[27]. Nielsen, S. H. H., Cunningham, F., Hay, R., Partington, G., & Stokes, M. (2015). 3D prospectivity modelling of orogenic gold in the Marymia Inlier, Western Australia. Ore Geology Reviews, vol. 71, pp. 578–591.

[28]. Chen, J., Lu, P., Wu, W., Zhao, J., & Hu, Q. (2007). A 3-D prediction method for blind orebody based on 3-D visualization model and its application. Earth Science Frontiers, vol. 14, no. 5, pp. 54–6 .

[29]. Xiao, K., Li, N., Porwal, A., Holden, E. J., Bagas, L., & Lu, Y. (2015). GIS-based 3D prospectivity mapping: a case study of Jiama copper-polymetallic deposit in Tibet, China. *Ore Geology Reviews, vol. 71*, pp. 611–632.

[30]. Reimann, C., Filzmoser, P., & Garrett, R.G. (2002). Factor analysis applied to regional geochemical data: problems and possibilities. *Appl. Geochem. 17* (3), 185–206.

[31]. Treiblmaier, H., & Filzmoser, P. (2010). Exploratory factor analysis revisited: how robust methods support the detection of hidden multivariate data structures in IS research. *Inf. Manag. 47* (4), 197–207.

[32]. Zuo, R. (2011). Identifying geochemical anomalies associated with Cu and Pb–Zn skarn mineralization using principal component analysis and spectrum–area fractal modeling in the Gangdese Belt, Tibet (China). *J. Geochem. Explor. 111*, 13–22.

[33]. Afzal, P., Eskandarnejad Tehrani, M., Ghaderi, M., & Hosseini, M.R. (2016). Delineation of supergene enrichment, hypogene, and oxidation zones utilizing SFA and fractal modeling in Takht-e-Gonbad porphyry deposit, SE Iran. *J. Geochem. Explor. 161*, 119–127.

[34]. Hoseinzade, Z., & Mokhtari, A.R. (2017). A comparison study on the detection of key geochemical variables and factors through three different types of factor analysis. *J. Afr. Earth Sci. 134*, 557–563.

[35]. Shamseddin Meigoony, M., Afzal, P., Gholinejad, M., Yasrebi, A.B., & Sadeghi, B. (2014). Delineation of geochemical anomalies using factor analysis and multifractal modeling based on stream sediments data in Sarajeh 1:100,000 sheet, Central Iran. Arab. *J. Geosci. 7*, 5333–5343.

[36]. Afzal, P., Heidari, S.M., Ghaderi, M., & Yasrebi, A.B. (2017). Determination of mineralization stages using correlation between geochemical fractal modeling and geological data in Arabshah sedimentary rock-hosted epithermal gold deposit, NW Iran. *Ore Geol. Rev. 91*, 278–295.

[37]. Yousefi, M., Kamkar-Rouhani, A., & Carranza, E.J.M. (2014). Application of SFA and logistic function to create a fuzzy stream sediment geochemical evidence layer for mineral prospectivity mapping. Geochem. Explor. *Environ. Anal. 14* (1), 45–58.

[38]. Mandelbrot, B.B. (1983). The Fractal Geometry of Nature. W.H. Freeman, San Francisco.

[39]. Cheng, Q., Agterberg, F.P., & Ballantyne, S.B. (1994). The separation of geochemical anomalies from background by fractal methods. *J. Geochem. Explor. 51*, 109–130.

[40]. Cheng, Q. (1999). Spatial and scaling modeling for geochemical anomaly separation. *J. Geochem. Explor. 65*, 175–194.

[41]. Li, C.J., Ma, T.H., & Shi, J.F. (2003). Application of a fractal method relating concentration and distances for the separation of a geochemical anomaly from the background. *J. Geochem. Explor. 77*, 167–175.

[42]. Afzal, P., Fadakar Alghalandis, Y., Khakzad, A., Moarefvand, P., & Rashidnejad Omran, N. (2011). Delineation of mineralization zones in porphyry Cu deposits by fractal concentration–volume modeling. *J. Geochem. Explor. 108*, 220–232.

[43]. Agterberg, F.P. (1995). Multifractal modeling of the sizes and grades of giant and supergiant deposits. Int. Geol. Rev. 37, 1–8.

[44]. Cheng, Q. (2008). Modeling local scaling properties for multiscale mapping. *Vadose Zone J.* 7, 525–532.

[45]. Zuo, R., Cheng, Q., & Xia, Q. (2009). Application of fractal models to the characterization of the vertical distribution of geochemical element concentration. J. Geochem. *Explor. 102*, 37–43.

[46]. Afzal, P., Fadakar Alghalandis, Y., Moarefvand, P., Rashidnejad Omran, N., & Asadi Haroni, H. (2012). Application of power-spectrum-volume fractal method for detecting hypogene, supergene enrichment, leached and barren zones in Kahang Cu porphyry deposit, Central Iran. J. Geochem. *Explor. 112*, 131–138 .

[47]. Afzal, P., Dadashzadeh Ahari, H., Rashidnejad Omran, N., & Aliyari, F. (2013). Delineation of gold mineralized zones using concentration-volume fractal model in Qolqoleh gold deposit, NW Iran. *Ore Geol. Rev. 55*, 125–133.

[48]. Afzal, P., Adib, A., & Ebadati, N. (2018). Delineation of seismic zonation using fractal modeling in West Yazd province, Central Iran. J. *Seismol. 22* (6), 1377–1393.

[49]. Hassanpour, S., & Afzal, P. (2013). Application of concentration–number (C–N) multifractal modeling for geochemical anomaly separation in Haftcheshmeh porphyry system, NW Iran. *Arab. J. Geosci. 6*, 957–970.

[50]. Aliyari, F., Afzal, P., & Abdollahi Sharif, J. (2017). Determination of geochemical anomalies and gold mineralized stages based on lithogeochemical data in the Zarshuran Carlin-like gold deposit (NW Iran) utilizing

multifractal modeling and SFA. J. *Mining Environ. 8* (4), 593–610.

[51]. Daneshvar Saein, L., & Afzal, P. (2017). Correlation between Mo mineralization and faults using geostatistical and fractal modeling in porphyry deposits of Kerman Magmatic Belt, SE Iran. J. Geochem. *Explor. 181*, 33–343.

[52]. Nazarpour, A. (2018). Application of C-A fractal model and exploratory data analysis (EDA) to delineate geochemical anomalies in the Takab 1:25,000 geochemical sheet, NW Iran. Iran. J. *Earth Sci. 10*, 173–180.

[53]. Ostadhosseini, A., Barati, M., Afzal, P., & Lee, I. (2018). Polymetallic mineralization prospecting using fractal and staged factor analysis in Ardestan area, Central Iran. *Geopersia 8*, 279–292.

[54]. Soltani, F., Moarefvand, P., Alinia, F., & Afzal, P. (2019). Characterizing Rare Earth Elements by coupling multivariate analysis, factor analysis, and geostatistical simulation; case-study of Gazestan deposit, central Iran. J. *Mining Environ. 10*, 929–945.

[55]. Yasrebi, A.B., & Hezarkhani, A. (2019). Resources classification using fractal modelling in Eastern Kahang Cu-Mo porphyry deposit, Central Iran. *Iran. J. Earth Sci. 11*, 56–67.

[56]. Ghannadpour, S. S. (2022). Delineation of mineralization zones in porphyry Cu deposits by fractal concentration–volume modeling. *Journal of Geochemical Exploration, 108*(3), 220-232.

[57]. Sadigh, S. (2023). Spatial distribution of porphyry copper deposits in Kerman Belt, Iran — Implications for exploration (fractal and fry analysis). *Earth Sciences Research Journal, 26*(4), 321-333.

[58]. Hezarkhani, A., & Williams-Jones, A.E. (1998). Controls of alteration and mineralization in the Sungun porphyry copper deposit, Iran: evidence from fluid inclusions and stable isotopes. *Economic Geology 93*, 651–670.

[59]. Alavi, M. (1994). Tectonics of the Zagros orogenic belt of Iran: new data and interpretations. *Tectono physics 229*, 211–238.

[60]. Berberian, M., & King, G.C. (1981). To ward sapaleo geography and tectonic evolution of Iran. *Canadian Journal of Earth Sciences 18*, 210–265.

[61]. Stocklin, J.O. (1977). Structural correlation of the Alpine ranges between Iran and Central Asia. Memoir Hors Service Societe Geologique France 8, 333–353.

[62]. Shahabpour, J., & Doorandish, M. (2008). Mine drainage water from the SarCheshmeh porphyry copper mine, Kerman, Iran. *Environmental Monitoring and Assessment 141*, 105–120.

[63]. Mehrpartou, M. (1993). Contributions to the geology, geochemistry, ore genesis, and fluid inclusion investigations on Sungun Cu–Mo porphyry deposit, northwest of Iran, Unpublished PhD Thesis. *University of Hamburg, Germany, 245 pp.*

[64]. Asghari, O., Hezarkhani, A., & Soltani, F. (2009). The Sungun porphyry copper deposit, Iran (based on fluid inclusion studies). Acta Geological Polonica 59 (1),93–109.

[65]. Solovov, A. P. (1990). Handbook on geochemical prospecting for useful minerals.

[66]. Ziaii, M., Doulati Ardejani, F., Ziaei, M., & Soleymani, A.A. (2012). Neuro-fuzzy modeling-based genetic algorithms for the identification of geochemical anomalies in mining geochemistry. Appl. Geochem. 27, 663–676.

[67]. Imamalipour, A., & Mousavi, R. (2018). Vertical geochemical zonation in the Masjed Daghi porphyry copper-gold deposit, northwestern Iran: implications for exploration of blind mineral deposits. Geochemistry: Exploration, Environment, Analysis, 18(2), 120-131.

[68]. Ziaii, M., Safari, S., Timkin, T., Voroshilov, V., & Yakich, T. (2019). Identification of geochemical anomalies of the porphyry-Cu–Cu deposits using concentration gradient modelling: a case study, Jebal-Barez area, Iran. J. Geochem. Explor. 199, 16–30.

[69]. Imamalipour, A., Karimlou, M., & Hajalilo, B. (2019.) Geochemical zonality coefficients in the primary halo of Tavreh mercury prospect, northwestern Iran: implications for exploration of listwaenitic type mercury deposits. Geochemistry: Exploration, Environment, Analysis, 19(4), 347-357.

[70]. Aliyari, F., Afzal, P., Lotfi, M., Shokri, S., & Feizi, H. (2020). Delineation of geochemical haloes using the developed zonality index model by multivariate and fractal analysis in the Cu–Mo porphyry deposits., Applied Geochemistry 121.

[71]. Filzmoser, P., Hron, K., & Reimann, C. (2009). Univariate statistical analysis of environmental (compositional) data: problems and possibilities. Sci. Total Environ. 407, 6100–6108.

[72]. David, M. (1977). Geostatistical Ore Reserve Estimation, Amsterdam: Elsevier, 283 p.

[73]. Lowell, J.D., & Guilbert, J.M. (1970). Lateral and vertical alteration-mineralization zoning in porphyry ore deposits. Economic Geology 65, 373–408.

انجمن مهندسی معدن ایران
نشریه مهندسی معدن و محیط زیست
نشانی نشریه: www.jme.shahroodut.ac.ir
دانشگاه صنعتی شاهرود

شاخص منطقه بندی ژئوشیمیایی سه بعدی براساس آنالیز فاکتوری مرحله‌ای و مدل‌سازی فراکتالی در کانسارهای پورفیری مس – مولیبدن

حسن فیضی انهر، علی امامعلی‌پور* و پیمان افضل

گروه مهندسی معدن، دانشکده فنی و مهندسی، دانشگاه ارومیه، ارومیه، ایران

اطلاعات مقاله

تاریخ ارسال: ۲۰۲۵/۰۹/۱۵
تاریخ داوری: ۲۰۲۵/۱۱/۰۲
تاریخ پذیرش: ۲۰۲۵/۱۲/۳۱

DOI: 10.22044/jme.2025.16830.3300

کلمات کلیدی

شاخص منطقه بندی ژئوشیمیایی سه بعدی توسعه یافته،
آنالیز فاکتوری مرحله‌ای
مدل فراکتالی
مس - مولیبدن پورفیری
مدلسازی سه بعدی

چکیده

منطقه بندی ژئوشیمیایی یکی از مفاهیم کلیدی در ژئوشیمی اکتشافی است که ابزاری کارآمد برای پیش‌بینی سطح فرسایش کانسار، تفکیک هاله‌های فوق کانساری از تحت کانساری، و شناسایی توده‌های کانساری پنهان فراهم می‌کند. اگرچه روش‌های کلاسیک منطقه بندی ژئوشیمیایی طی دهه‌های گذشته به‌طور گسترده مورد استفاده قرار گرفته‌اند، این پژوهش یک مدل بهبودیافته منطقه بندی ژئوشیمیایی سه‌بعدی را ویژه کانسار پورفیری سونگون معرفی می‌کند که بر پایه داده‌های ژئوشیمیایی حاصل از ۲۶۴ گمانه حفاری شامل ۳۳٬۳۶۸ نمونه سنگی توسعه یافته است. این مدل با استفاده از نسبت فاکتورهای استخراج‌شده از آنالیز فاکتوری مرحله‌ای عناصر اصلی مرتبط با عناصر کانی‌زایی (مس و مولیبدن) و عناصر فرعی (کادمیم، منگنز، سرب، روی و نقره) ساخته شده و سپس به‌منظور طبقه‌بندی دقیق‌تر، با مدل‌سازی فراکتالی بهبود یافته است. نتایج مدل‌سازی فراکتالی به روش فرکتالی عیار – حجم به‌وضوح وجود چهار جامعه مجزا و سه نقطه شکست را نشان می‌دهد که به ترتیب معرف زون‌های سوپرژن (۰٫۹ تا ۱٫۴ درصد)، هیپوژن (۰٫۶ تا ۰٫۹ درصد) و زون اکسیداسیون (۰٫۱ تا ۰٫۶ درصد) هستند. کاربرد این روش در سیستم پورفیری سونگون، همبستگی فضایی قوی میان شاخص منطقه بندی، توزیع عیار مس و الگوهای دگرسانی را نشان می‌دهد. آنالیز فاکتوری مرحله‌ای توانایی بالایی در تفکیک عناصر فوق کانساری و تحت کانساری دارد، در حالی که مدل‌سازی فراکتالی موجب افزایش پایداری و اطمینان‌پذیری منطقه بندی می‌شود. تلفیق شاخص منطقه بندی سه‌بعدی توسعه‌یافته با مدل‌های عیار مس، ارتباط ساختاری روشنی میان دگرسانی، نسبت‌های ژئوشیمیایی و توزیع مس آشکار می‌سازد. رویکرد پیشنهادی با افزایش قدرت تفکیک منطقه بندی در کانسارهای پورفیری، دقت هدف‌گذاری اکتشافی را بهبود بخشیده و ریسک حفاری‌های عمیق اکتشافی را کاهش می‌دهد.

نویسنده مسئول مکاتبات: a.imamalipour@urmia.ac.ir (ع. امامعلی‌پور)